Damage Detection of Carbon Fiber-reinforced Concrete Under Bending Test

Rooholla Kamani, Mehdi Kamali Dolatabadi*, Ali Asghar Asgharian Jeddi, and Kourosh Nasrollahzadeh

***Abstract*- Nowadays, fiber-reinforced concrete plays a vital role in the construction industry due to its superior mechanical properties, corrosion resistance, and light weight characteristics.Thanks to the partial penetration of fine-grained concrete within the bundle of fibers, ductile behavior of fiber-reinforced concrete can be anticipated. In this capacity, the bundle of fibers is divided into two distinct areas namely, the fibers embedded into concrete,which is called as sleeve fibers, and dry fibers which are supposed to behave as core fibers. Accordingly, estimating the number of sleeve fibers and distinguishing their damages when the fiber-reinforced concrete is subjected to load service are the main scopes of this study. Electrical resistance of roving was measured by Wheatstone bridge technique to detect fiber damage during bending of fiber-reinforced concrete beam. Besides, the number of sleeve fibers on the roving cross-section was estimated using SEM images and was correlated with the changes in the electrical resistance of roving. The results indicate that the sleeve fibers fail with a distinctive delay after the occurrence of the first crack, while the core fibers remain sound. Eventually, it is demonstrated that the proposed methodis capable of estimating the number of damaged fibers during bending test, and also evaluating the penetration of the cement matrix within the bundle of fibers.**

***Keywords*: fiber-reinforced concrete; damage detection; electrical resistance, carbon fibers**

I. INTRODUCTION

R. Kamani, M.K. Dolatabadi
Department of Textile Engineering, Science and Research Branch, Islamic Azad University, Tehran, Iran.

A.A. Asgharian Jeddi
Department of Textile Engineering, Amirkabir University of Technology, Tehran, Iran.

K. Nasrollahzadeh
Department of Civil Engineering, Khajeh Nassir-Al-Deen Toosi, University of Technology, Tehran, Iran.

Correspondence should be addressed to M.Kamali Dolatabadi
e-mail: kamalimehdi@yahoo.com

Fiber-reinforced concrete (FRC) is largely used to construct thin and light weight walls or surfaces and can provide a highload−bearing capacity. The main advantages of FRCs are high specific strength, durability and unique characteristics resulted from the presence of fibers with different structures and orientations (Dolatabadi *et al.*, 2014; Hegger *et al.*, 2008). The most common fibers with variety of structures used in the reinforced concretes include polypropylene (PP), polyethylene (PE), alkali resistant (AR) glass, carbon and Kevlar fibers (Peled & Bentur, 2003). Many factors influence on the properties of FRC, such as type of fiber, concrete permeability within the bundle of fibers, reinforcement interface, curing conditions, reinforcement orientation, configuration, etc. (Colombo, 2013). Mechanical properties and efficiency of fibers in concrete depend on penetration of concrete within the bundle of fibers. The bundles of fiber sembedded in concrete are divided into two distinct groups: firstly, the fibers that are bonded directly to concrete, the so-called sleeve fibers, and secondly, the fibers that lay in core of roving without any cementitious matrix between them. The sleeve fibers may experience rupture due to crack opening when an FRC beam is subjected to the tensile stresses. However, the core fibers remain without breakage and may just slid against the external fibers during opening of the crack. This sliding of fibers, which is known as telescopic phenomena, causes the ductile behavior of FRCs under deflection. Consequently, the energy absorption of FRCs during bending test can be increased due to the mentioned telescopic phenomena (Cohen & Peled, 2010; Dolatabadi, 2011).

Reliability of FRC structures and providing control on the safety level of such a thin structure are of great importance and interest. Damage detection allows to reveal some deficiency to avoid any sudden damage or deterioration (Materazzi *et al.*, 2013; Ding *et al.,* 2013; Han *et al.*, 2015; Doweny *et al.*, 2017). Major or minor damages might occur in the structure due to overload, earthquake, wind, fatigue, etc. Major damage in concrete is visible by

cracks, and can be recognized by some techniques like visual inspection, liquid penetrant, ultrasonic, etc. Minor damage detection is much more challenging than major damage detection. The use of sensors, such as optical fibers and acoustic technique can be employed to detect FRC damage. However, some disadvantages may be encountered when applying sensors for instance; high cost, low durability, and small sensing volume (Bontea *et al.*, 2000; Chen & Liu 2008).

A method for monitoring the minor and major damages at the real failure time by electrical resistance of chopped carbon fibers has been proposed by Chen & Chung (1996). In this method, an appropriate volume of carbon fiber could form a conductive network in concrete. It is then expected that the resistivity of carbon fiber-reinforced concrete changes based upon the imposed strain. It is obvious that the electrical resistivity depends on the strain. Afterwards, the electrical resistance measurement of short carbon fiber-reinforced concrete has been employed for several applications (Shi *et al.*, 1999; Chung 2000; Chen *et al.,* 2017; Azhari *et al.*, 2017).

Wen et al. (2007) discussed the ability of self–monitoring of damage by the use of short carbon fibers inside the reinforced concrete. The electromechanical damage-sensing behaviors of steel fiber-reinforced concrete at different strain hardening rates and various stress amplitudes are compared as well (Nguyen *et al.*, 2015). To measure electrical resistance of carbon/glass roving-reinforced concrete under cyclic loads in the un-cracked region, Wheatstone bridge has been applied (Goldfield *et al.* 2016). Quadflieg *et al.* (2016) used carbon rovings instead of embedded strain sensors for structural health monitoring. The problem with relying on the conductivity of carbon roving is that all fibers are connected to each other. As a consequence of this inter-connection among fibers under damage conditions, electrons transfer to neighboring fibers, which in turn, is dependent on energy resources. That is why the accurate way to measure the small changes of carbon roving structure when it is used as sensors, is Wheatstone bridge method with an independent power supply.

Recently, the flexural behavior of concrete reinforced with carbon fibers has been studied by Kamani *et al.* (2017). It is demonstrated that the penetration of cementitious matrix within the bundle of fibers is a key factor which affects the bending behavior of such beams. The penetration of cement within the bundle of fibers can be deducted by the method proposed in this paper.

The main objective of the current paper is to measure the electrical resistance of carbon fibers (ERCF) embedded in reinforced concretes under large deformation simposed to the beams using Wheatstone bridge method. To this aim, the change in ERCF after cracking is determined and considered to be related to the cement matrix penetrationas well as the broken fibers.

II. EXPERIMENTAL PROGRAM

A. Fine-grained concrete properties

Fine-grained concrete used in this study contained Portland cement (I), silica fume, a polycarboxylate-based superplasticizer, and sand (see Table I). The mixing method was such that the sand and binders were blended together as dry materials whereas water and superplasticizer were mixed as liquid materials, separately. Afterwards, liquid materials were gradually added to the dry materials and mixed to achieve a homogeneous concrete. Then, the mixture was vibrated for 5 min to let the bubbles get out.

The average compressive strength of five identical samples of concrete cured after 28 days was measured as 83.33 MPa (with a standard deviation of 3.06) according to ASTM 30109.

TABLE I
COMPOSITION OF FINE-GRAINED CONCRETE

Portland cement (I)	Silica fume	Superplasticizer	Water		Siliceous Fine sand (0-0.125 mm)	Siliceous Sand (0.125-0.6 mm)
				Water/ cement		
kg/m^3	kg/m^3	kg/m^3	kg/m^3	-	kg/m^3	kg/m^3
650	65	16	255	0.375	500	714

TABLE II
CARBON FIBER SPECIFICATIONS

Trade name	Number of Fibers	Tensile Strength	Tensile Modulus	Strain	Density	Sizing Type & Amount	Specific Heat	Filament Diameter
-	numbers	MPa	GPa	%	g/cm^3	E & %	Cal/g°C	μm
Torayca	12000	4900	230	2.1	1.80	60&0.3	0.18	7

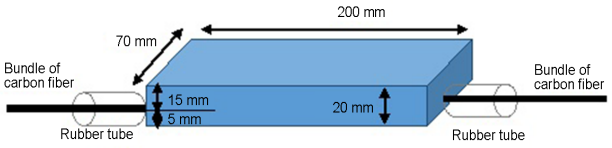

Fig. 1. Sample preparation details.

B. Carbon fiber specifications

The carbon roving was utilized as the reinforcementof the specimens under study. The specifications of carbon fibersare summarized in Table II.

C. Preparation of test samples

Rectangular molds with dimensions of 200*70*20 mm were used for casting the samples (Fig. 1). A roving was fixed at 5 mm from the bottom of the mold in order to be assured that it is located in the tensile region of the bending bars. Afterwards, the prepared concrete was poured into the molds while the roving kept at the above-mentioned position. A rubber tube was applied on both sides of the sample to protect the brittle carbon fibers against molding and demolding process (see Fig. 1). The samples were demolded after 24 h and then, were exposed to 100% relative humidity at room temperature for 28 days to ensure the complete cement hydration.

After that, the rubber tube was removed, and all the fibers at both ends of the sample were placed on a sheet of copper. Two terminals were used in the both sides of the sample for fixing the copper sheet with all the fibers and a connection wire. The connection wire length was one meter with negligible resistance. Five sample beams reinforced with fibers were prepared following the above-mentioned procedure along with three additional unreinforced samples as reference beams.

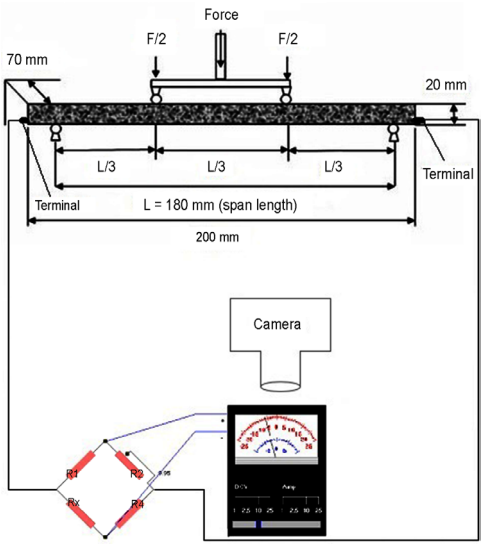

Fig. 2. Test setup (a) four–point bending (b) measurement of ERCF setup.

D. Bending test setup and Wheatstone bridge method

Four-point bending tests were carried out by use of a Zwick's testing machine (type 1494). A load cell with a 10 kN capacity was used, and the span length of the beams was considered as 180 mm (Fig. 2(a)). The loading speed was set at 5 mm/min.The load−deflection curves of the tested beams and the electrical resistance of carbon roving for each sample were measured and recorded simultaneously. Fig. 2 depicts the test setup of this study.

One of the accurate ways to measurean unknown resistance independent fromthe power supply is the Wheatstone bridge method. The Wheatstone bridge method has been applied to measurement of small changes in the resistance in several investigations (Hoffmann, 2016). The details of Wheatstone bridge (Pontavi WH2) arrangement is indicated in Fig. 2 (b), where R_x is the unknown resistance (here, carbon roving resistance), R_1 and R_3 are the resistors with constant resistance values, and the resistance of R_2 is adjustable (i.e., variable resistance). If the ratio of the two resistances, in the known leg (R_2/R_1) is equal to the ratio of the second leg (R_X/R_3), the voltage between the two midpoints (B and D) will be zero, and no current will flow through the galvanometer V_G. The variable resistor (R_2) must be adjusted to leading negligible current between B and D points. In this condition, the galvanometer will be show the zero value. Accordingly, one can conclude that (Blatt & LaBrecque, 1988):

$$I_1R_1 = I_2R_3 \tag{1}$$

$$I_1R_2 = I_2R_X \tag{2}$$

$$R_X = \left(\frac{R_2}{R_1}\right).R_3 \tag{3}$$

Where, I_1: electrical current between R_1-R_2, I_2: electrical current between $R_{3-}R_x$.

In this way, the value of the resistor (R_2) was changed manually during bending test until the value of the galvanometer (V_G) became zero and the value of the resistor was recorded by a camera, simultaneously. Afterwards, the values of variable R_x were read, while the VGwas equal tozero. By this manner, the R_x was calculated using Eq. (3) for a certain time during the bending test.

E. Measurement of the number of Sleeve fibers by image-processing technique

In order to investigate the position of fibers in concrete and estimate the number of sleeve and core fibers, SEM photographs were prepared from the cross − section of

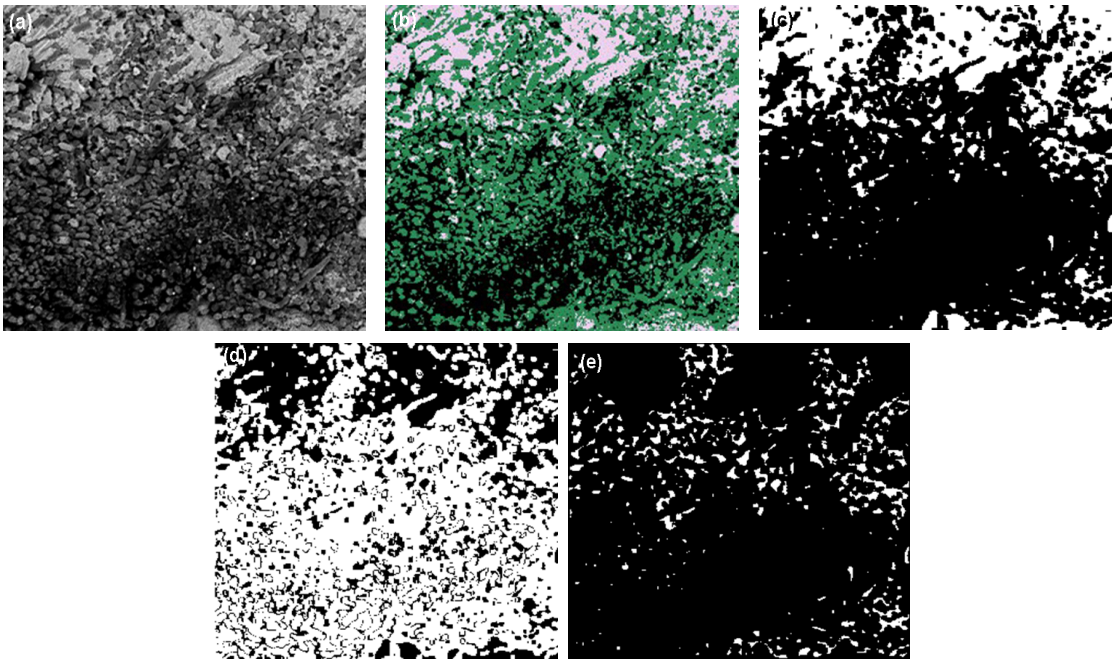

Fig. 3. (a): Original image of section 1 segment 1, (b): discriminating three classes, fiber (green), concrete (white) gap (black) (c): concrete, (d): total fiber, and (e): sleeve fiber pixels.

concrete reinforced with the bundle of fibers after bending test. For each sample, three cross−sections area aligned as a cubic with dimension of 1*1*1cm in such way that roving fibers were located in the center of cross−section. By considering the ribbon shape and size of the roving cross−section, each cross−section was scanned by taking at least two images at 200× magnitude. Eventually, to apply image-processing technique, six images were taken for cross−section of each sample.

Two steps were considered to detect sleeve fibers. First: to discriminate fibers, concrete and gaps the minimum distance classification method was applied on the taken images using ENVI software. Several train data were selected from each class, after that the considered image was classified by this method (Wacker, 1972; Mather *et al.*, 2016). Second: to detect the sleeve fibers, a filter was applied on concrete class data and afterwards the interface of fibers class and concrete class data was considered as percent of sleeve fibers using MATLAB codes. Fig. 3 shows this process for an image in details.

III. RESULTS AND DISCUSSIONS

A. Flexural properties of beam samples

Flexural properties were calculated from the load−displacement curve of four-point bending test in this study. The area under load−displacement curveis defined as toughness. The bearing load at the occurrence of the first crack (f_{cr}), the displacement at the first crack (δ_{cr}), the toughness up to the first crack (A_{cr}), the flexural strength ($Б_{cr}$), the flexural modulus of elasticity (E), the maximum displacement (δ_{ult}), the toughness up to maximum displacement (A_{ult}) of samples are presented in Table III.

There is no significant difference at the level of 95% between the flexural properties of reinforced samples and unreinforced specimens at the first crack (Table III). Nevertheless, the failure mechanism of reference samples was catastrophic, and the reference samples failed in a brittle manner after the first crack. However, the reinforced samples exhibited flexural resistance after the first crack. Consequently, a significant difference (at the level of 99%) between the behaviors of reinforced and unreinforced specimens was observed mainly at the maximum displacement and maximum toughness (i.e., δ_{ult} and A_{ult}). It is recognized that the fibers which were broken (damaged) after the first crack could not give enough strengthening to the concrete due to lack of reinforcement. However, to detect damaged fibers and the failure mechanism of the reinforced concrete beam, one remaining roving was adequate.

Indeed, fibers bridge the crack (s) and the failure mechanisms are in such a way that fibers resist the applied loads up to breakage of sleeve fibers followed by sliding of unbroken fibers. Therefore, energy absorption of the strengthened samples is larger than that of the reference samples. Obviously, the deflection of the strengthened sample is higher than that of the reference sample too.

TABLE III
MECHANICAL PROPERTIES OF DIFFERENT SAMPLES

Sample	f_{cr}(N)	δ_{cr}(mm)	A_{cr}(N.mm)	$Б_{cr}$(MPa)	E(GPa)	δ_{ult}(mm)	A_{ult}(N.mm)
Sample 1	795.02	0.52	156.40	5.66	3.44	5.00	992.08
Sample 2	962.71	0.58	195.38	6.86	3.73	4.85	839.45
Sample 3	756.20	0.62	167.85	5.39	2.74	5.00	740.25
Sample 4	857.92	0.54	136.03	6.11	3.57	3.60	630.72
Sample 5	862.82	0.51	141.91	6.15	3.81	4.94	612.46
Ave. Sample	846.93(73.42)*	0.554(0.04)*	159.51(21.68)*	6.03(0.52)*	3.46(0.39)*	4.68(0.61)*	667.21(157.32)*
Reference 1	711.57	0.54	154.23	5.07	2.96	0.56	161.32
Reference 2	770.94	0.55	157.90	5.49	3.15	0.58	168.38
Reference 3	795.02	0.56	171.68	5.66	3.19	0.59	188.27
Ave. Ref	759.17(42.95)*	0.549(0.01)*	161.27(9.20)*	5.41(0.30)*	3.10(0.12)*	0.58(0.01)*	172.68(13.97)*

*Standard deviation
f_{cr}: Bearing load at first−crack, δ_{cr}: Displacement at first− crack, A_{cr}: Toughness up to first−crack, $Б_{cr}$: Flexural strength, E: Flexural modulus of elasticity, δ_{ult}: Maximum displacement, Ault: Ultimate toughness

TABLE IV
ERCF CHANGES IN DIFFERENT SECTIONS

Sample	$Rate_I$ of change in ERCF	$\Delta R_I(\Omega)$	$Time_I$ (sec.)	$Rate_{II}$ of change in ERCF	$\Delta R_{II}(\Omega)$	$Time_{II}$ (sec.)	$Rate_{III}$ of change in ERCF	$\Delta R_{III}(\Omega)$	$Time_{III}$ (sec.)
Sample 1	0.005	0.10	20.43	0.078	2.30	50.09	0.012	1.50	178.67
Sample 2	0.010	0.20	20.32	0.073	1.90	46.41	0.020	2.00	144.18
Sample 3	0.005	0.10	17.85	0.110	1.80	34.22	0.021	1.40	120.07
Sample 4	0.005	0.10	20.37	0.178	1.80	30.48	0.025	2.20	110.73
Sample 5	0.009	0.20	21.64	0.115	1.60	35.53	0.020	2.20	146.65
Average	0.007(0.002)*	0.14(0.05)*	20.12(1.38)*	0.111(0.042)*	1.88(0.26)*	39.35(8.44)*	0.020(0.005)*	1.86(0.38)*	140.06(26.51)*

*Standard deviation

B. Electrical resistance of bundle of carbon fibers

The ERCF for different samples was recorded simultaneously during bending test by Wheatstone bridge. The ERCF versus time curves for specimens are depicted in Fig. 4 Divergences of ERCF versus time curves of specimens could be attributed to the different moisture content of fibers and penetration of cement as well. Clearly,

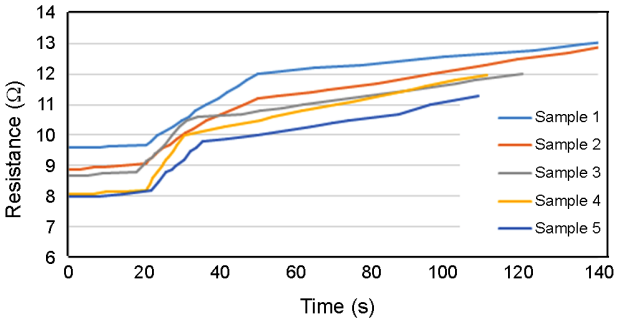

Fig. 4. ERCF versus time curves for different samples.

each ERCF curve consists of three regions. Tiny change in ERCF was observed at the first section that is related to small extension of fibers, then, the ERCF raised rapidly due to breakage of sleeve fibers at the second section, and finally, the ERCF changed moderately due to sliding of fibers at the third section. To eliminate the influence of fiber moisture, the difference of mutual electrical resistance (ΔR) and rates of change in ERCF for each of three sections was computed. These values are presented in Table IV.

C. Synchronizing of bending data and ERCF measurement

The load−displacement of bending test and ERCF at the same time are synchronized for the first sample, as typically shown in Fig. 5. According to the diagram, major changes in ERCF occur just several seconds after the first crack. This delay refers to confrontation of fibers against crack opening.

The averagerates of change in ERCF for three regions

TABLE V
COMBINATION OF BENDING AND ELECTRICAL TEST DATA

Sample	Region I		Region II		Region III	
	δ_I (mm)	A_I (N.mm)	δ_{II} (mm)	A_{II} (N.mm)	δ_{III} (mm)	A_{III}(N.mm)
Sample 1	0.68	268.33	1.68	479.49	5	179.61
Sample 2	0.67	192.00	1.55	289.76	4.85	357.69
Sample 3	0.59	165.36	1.10	116.42	5	458.46
Sample 4	0.55	169.70	0.89	93.04	3.6	367.98
Sample 5	0.73	178.03	1.19	38.64	4.94	395.78
Average	0.64(0.07)*	194.69(42.40)*	1.28(0.33)*	203.47(180.67)*	4.68(0.61)*	351.90(103.99)*

*Standard deviation

TABLE VI
ESTIMATED SLEEVE AND CORE FIBERS

sample	Average of sleeve fibers pixels (%)	Number of sleeve fibers	Average of core fibers pixels (%)	Number of core fibers
Sample1	12.47	1496	87.53	10503
Sample2	7.06	847	92.94	11153
Sample3	6.08	729	93.92	11270
Sample4	6.29	755	93.71	11245
Sample5	5.71	685	94.29	11314
Average	7.52(2.08)*	902(337.16)*	92.00(2.81)*	11097(337.16)*

*Standard deviation

were 0.007, 0.111 and 0.020 Ω/s, respectively. The deflection and toughness of the bending load−deflection curves based on the ERCF at three regions are summarized in Table V.

Damage of sleeve fibers would be occurred from the beginning of region II. Therefore, it is anticipated that the bending toughness in this region would be correlated with the difference of mutual electrical resistance (ΔR). Fig. 6 gives a graph of this correlation. One can deduce that the ΔR in region II is sensitive to rupture of fibers.

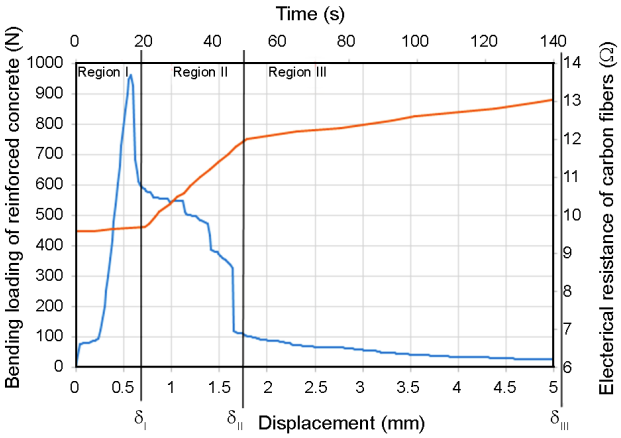

Fig. 5. Synchronizing bending load−displacement and ERCF−time.

D. Sleeve fibers measuring

The number of sleeve fibers and core fibers for each sample are presented in Table VI. The main question is whether the sleeve fibers and then the penetration of cement matrix can be computed by the ERCF test results.

E. Calibrating ERCF test and number of broken fibers

Fig. 7 indicates the relationship between the ΔR of ERCF in the region II and the sleeve fibers value with high correlation. As a result, the greater is the penetration of cement particles into the bundle of fibers, the higher ΔR

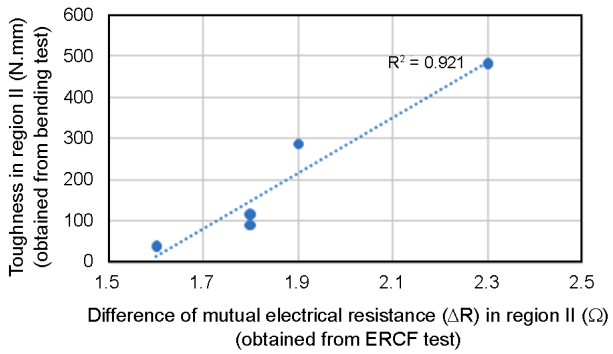

Fig. 6. Correlation between the ΔR and bending toughness in region II.

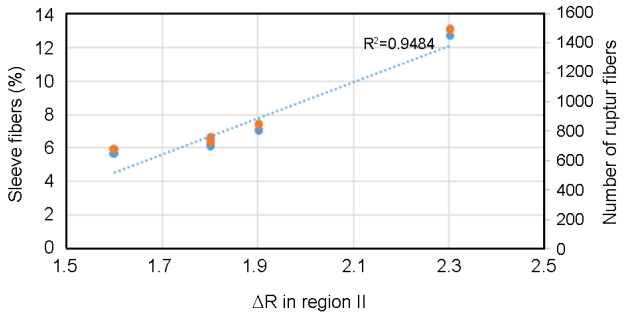

Fig. 7. Relationship betweenthe sleeve fibers and ΔR of ERCF in region II.

is observed. Based on current knowledge, there is partially cement matrix penetration within bundle of fibers, which the embedded fibers (sleeve fibers) are subjected to damage during bending test just after the first crack. On the other hand, assessing the cement matrix penetration and number of sleeve fibers is time consuming and it is not acost effective method. Accordingly, ERCF method can be applied to evaluate the penetration of cement matrix as well.

IV. CONCLUSIONS

Detecting damage fiber was addressed in this paper using ERCF test during bending deformation. It was found that change in ERCF during bending deformation of FRC consisted of three different regions. The average rates of change in ERCF for three regions were 0.007, 0.111 and 0.020 Ω/s, respectively. The major changes in ERCF occurred with a distinct delay after the first crack. It was demonstrated that the fiber damaging had been started in these regions. The sleeve fibers embedded directly in concrete were subjected to rupture during bending deformation of samples. The number of sleeve fibers was measured by applying image processing on SEM images taken from several cross-sections. The image processing test result showed the average percentage of sleeve fibers was 8% and the average percentage of the core fibers was 92%. The number of damaged fibers was correlated with the ΔR of ERCF test in the region II, and these values were verified by measuring bending toughness in the region II, and the sleeve fibers data were evaluated as well. Finally, it was shown that not only the ERCF test method was sensitive to compute the number of damaged fibers during bending deformation of FRC beams, but also it was capable to evaluate sleeve fibers and cement matrix penetration within the bundle of fibers.

REFERENCES

[1] F. Azhari and N. Banthia, "Carbon fiber-reinforced cementitious composites for tensile strain sensing", *ACI Mater. J.*, vol. 114, no. 1, 2017.

[2] F.J. Blatt and R. La Brecque, "Principles of physics", *Phys. Teach.*, vol. 26, no. 4, pp. 252-253, 1988.

[3] D.M. Bontea, D.D. L. Chung, and G.C. Lee, "Damage in carbon fiber-reinforced concrete, monitored by electrical resistance measurement", *Cem.Concr. Res.*, vol. 30, no. 4, pp. 651-659, 2000.

[4] B. Chen and J. Liu, "Damage in carbon fiber-reinforced concrete, monitored by both electrical resistance measurement and acoustic emission analysis", *Constr. Build. Mater.*, vol. 22, no. 11, pp. 2196-2201, 2008.

[5] P.W. Chen and D.D.L. Chung, "Carbon fiber reinforced concrete as an intrinsically smart concrete for damage assessment during static and dynamic loading", *ACI mater. J.*, vol. 93, no. 4, 1996.

[6] M. Chen, P. Gao, F. Geng, L. Zhang, and H. Liu, "Mechanical and smart properties of carbon fiber and graphite conductive concrete for internal damage monitoring of structure", *Constr. Build. Mater.*, vol. 142, pp. 320-327, 2017.

[7] D.D.L. Chung, "Cement reinforced with short carbon fibers: a multifunctional material", *Compos. Part B: Eng.*, vol. 31, no. 6, pp. 511-526, 2000.

[8] Z. Cohen and A. Peled, "Controlled telescopic reinforcement system of fabric–cement composites Durability concerns", *Cem. Concr. Res.*, vol. 40, no. 10, pp. 1495-1506, 2010.

[9] I.G. Colombo, A. Magri, G. Zani, M. Colombo, and M. Di Prisco, "Erratum to: textile reinforced concrete: experimental investigation on design parameters", *Mater. Struct.*, vol. 46, no. 11, pp. 1953-1971, 2013.

[10] Y. Ding, Z. Chen, Z. Han, Y. Zhang, and F. Pacheco-Torgal, "Nano-carbon black and carbon fiber as conductive materials for the diagnosing of the damage of concrete beam", *Constr. Build. Mater.*, vol. 43, pp. 233-241, 2013.

[11] M.K. Dolatabadi, S. Janetzko, and T. Gries, "Geometrical and mechanical properties of a non-crimp fabric applicable for textile reinforced concrete", *J. Text. Inst.*, vol. 105, no. 7, pp. 711-716, 2014.

[12] M.K. Dolatabadi, S. Janetzko, T. Gries, B.G. Kang, and A. Sander, "Permeability of AR-glass fibers roving embedded in cementitious matrix", *Mater. Struct.*, vol. 44, no. 1, pp. 245-251, 2011.

[13] Y. Goldfeld, S. Ben-Aarosh, O. Rabinovitch, T. Quadflieg, and T. Gries, "Integrated self-monitoring of carbon based textile reinforced concrete beams under repeated loading in the un-cracked region", *Carbon*, vol. 98, pp. 238-249, 2016.

[14] B. Han, S. Ding, and X. Yu, "Intrinsic self-sensing concrete and structures: A review", *Measure*., vol. 59, pp. 110-128, 2015.

[15] J. Hegger, M. Zell, and M. Horstmann, "Textile reinforced concrete-realization in applications", In: *Proceedings of International Fibre Symposium Tailor Made Concrete Structures: New Solutions for Our Society*, pp. 357-362, 2008.

[16] K. Hoffmann, "Applying the wheatstone bridge circuit", 2016, Available on :http://www.hbm.com.pl/pdf/w1569.pdf

[17] R. Kamani, M. Kamali Dolatabadi, and A.A. Jeddi, "Flexural design of textile-reinforced concrete (TRC) using warp-knitted fabric with improving fiber performance index (FPI)", *J. Text. Inst.*, vol. 109, no. 4, pp. 492-500, 2018.

[18] P. Mather andB. Tso, "Classification methods for remotely sensed data", *CRC*, 2016.

[19] A.L. Materazzi, F. Ubertini, and A. D'Alessandro, "Carbon nanotube cement-based transducers for dynamic sensing of strain", *Cem. Concr. Compos.*, vol. 37, pp. 2-11, 2013.

[20] D.L. Nguyen, J. Song, C. Manathamsombat, and D.J. Kim, "Comparative electromechanical damage-sensing behaviors of six strain-hardening steel fiber-reinforced cementitious composites under direct tension", *Compos. Part B: Eng.*, vol. 69, pp. 159-168, 2015.

[21] A. Peled and A. Bentur, "Fabric structure and its reinforcing efficiency in textile reinforced cement composites", *Compos. Part A: Appl. Sci. Manuf.*, vol. 34, no. 2, pp. 107-118, 2003.

[22] T. Quadflieg, O. Stolyarov, and T. Gries, "Carbon rovings as strain sensors for structural health monitoring of engineering materials and structures", *J. Strain Anal. Eng. Des.*, vol. 51, no. 7, pp. 482-492, 2016.

[23] Z.Q. Shi and D.D.L. Chung, "Carbon fiber-reinforced concrete for traffic monitoring and weighing in motion", *Cem. Concr. Res.*, vol. 29, no. 3, pp. 435-439, 1999.

[24] S. Wen and D.D.L. Chung, "Electrical-resistance-based damage self-sensing in carbon fiber reinforced cement", *Carbon*, vol. 45, no. 4, pp. 710-716, 2007.

[25] A.G. Wacker and D.A. Landgrebe, "Minimum distance classification in remote sensing", *LARS Tech. Rep.*, vol. 25, 1972.